© 2020. Published by The Company of Biologists Ltd | Journal of Experimental Biology (2020) 223, jeb223925. doi:10.1242/jeb.223925

RESEARCH ARTICLE

Pygmy mouse songs reveal anatomical innovations underlying acoustic signal elaboration in rodents

Tobias Riede[1,*] and Bret Pasch[2]

ABSTRACT

Elaborate animal communication displays are often accompanied by morphological and physiological innovations. In rodents, acoustic signals used in reproductive contexts are produced by two distinct mechanisms, but the underlying anatomy that facilitates such divergence is poorly understood. 'Audible' vocalizations with spectral properties between 500 Hz and 16 kHz are thought to be produced by flow-induced vocal fold vibrations, whereas 'ultrasonic' vocalizations with fundamental frequencies above 19 kHz are produced by an aerodynamic whistle mechanism. Baiomyine mice (genus *Baiomys* and *Scotinomys*) produce complex frequency-modulated songs that span these traditional distinctions and represent important models to understand the evolution of signal elaboration. We combined acoustic analyses of spontaneously vocalizing northern pygmy mice (*Baiomys taylori*) in air and light gas atmosphere with morphometric analyses of their vocal apparatus to infer the mechanism of vocal production. Increased fundamental frequencies in heliox indicated that pygmy mouse songs are produced by an aerodynamic whistle mechanism supported by the presence of a ventral pouch and alar cartilage. Comparative analyses of the larynx and ventral pouch size among four additional ultrasonic whistle-producing rodents indicated that the unusually low 'ultrasonic' frequencies (relative to body size) of pygmy mice songs are associated with an enlarged ventral pouch. Additionally, mice produced shorter syllables while maintaining intersyllable interval duration, thereby increasing syllable repetition rates. We conclude that while laryngeal anatomy sets the foundation for vocal frequency range, variation and adjustment of central vocal motor control programs fine tunes spectral and temporal characters to promote acoustic diversity within and between species.

KEY WORDS: Vocal production, Mammals, Geometric morphometrics, Contras-enhanced micro-CT, Ultrasonic vocalization

INTRODUCTION

Advertisement signals used in reproductive contexts are among the most diverse and elaborate traits in the animal kingdom (Bradbury and Vehrencamp, 2011). Understanding the mechanisms of signal production is central to understanding how signals diversify and the anatomical innovations that promote or constrain divergence. Indeed, recent work on traits used in social communication provides important insights into the processes underlying phenotypic evolution (e.g. Ord et al., 2013; Eliason et al., 2015, 2020).

Rodents produce diverse and complex vocal communication signals in a variety of social interactions (Sales and Pye, 1974; Brudzynski, 2018; Dent et al., 2018). Many muroid rodents are able to produce two distinct spectral ranges using divergent physical mechanisms (e.g. Pasch et al., 2017). Currently, sounds with spectral properties between 500 Hz and 16 kHz (hereafter 'audible sounds') are assumed to be produced by flow-induced vocal fold vibrations, whereas sounds with fundamental frequencies between 19 and 100 kHz (hereafter 'ultrasonic vocalizations', USV) are produced by a whistle mechanism (Riede, 2018). This distinction is based on data from laboratory mice (*Mus musculus*) and rats (*Rattus rattus*) and does not properly reflect the large acoustic diversity among non-traditional rodent models (e.g. Miller and Engstrom, 2007, 2010; Pasch et al., 2011, 2017). The spectral boundary between the two production mechanisms may not be as clear or mutually exclusive. Comparative data on vocal anatomy and underlying production mechanisms are thus needed to provide insight into the evolution of acoustic communication within the largest mammalian clade.

Current understanding of rodent vocal production mechanisms indicates that spectral content is determined by laryngeal anatomy (Riede, 2018). Ultrasonic whistle production appears to be dependent upon the presence of an intra-laryngeal air sac (ventral pouch) as well as a small cartilage (alar cartilage) that supports the ventral pouch entrance (Riede et al., 2017). The ventral pouch and the alar cartilage are located rostral from the vocal folds and have been identified in a few muroid rodents (laboratory mouse: *Mus*, laboratory rat: *Rattus*, and grasshopper mouse; *Onychomys*: Riede et al., 2017). However, both structures were absent in a heteromyid rodent (kangaroo rat: *Dipodomys*) that displays a limited vocal repertoire (Riede et al., 2017). Indeed, alterations of the ventral pouch cause changes in or disappearance of ultrasonic vocal capabilities (Riede et al., 2017). Furthermore, muscle activity can regulate the position of the alar cartilage and ventral pouch size to modulate spectral features of vocalization (Riede, 2013). Altogether, the ventral pouch appears to be critical for ultrasonic whistle production and its size is predicted to be negatively associated with the fundamental frequency of vocalizations (Riede et al., 2017).

Cricetid rodents in the subfamily Neotominae commonly produce audible (<20 kHz) vocalizations (Miller and Engstrom, 2007, 2010). Animals often assume an upright posture and open their mouths widely to generate loud vocalizations (Bailey, 1931; Blair, 1941; Packard, 1960; Hooper and Carleton, 1976), which are used to attract mates and repel rivals (Campbell et al., 2019; Pasch et al., 2011, 2013). Northern pygmy mice (*Baiomys taylori*) are crepuscular cricetid rodents that inhabit arid grasslands, coastal prairie mixed scrub, post oak savanna, and mesquite–cactus habitats from Texas to Mexico (Eshelman and Cameron, 1987; Light et al., 2016; Packard, 1960; Carleton, 1980). The staccato-like song of

[1]Department of Physiology, Midwestern University, Glendale, AZ 85308, USA. [2]Department of Biological Sciences, Northern Arizona University, Flagstaff, AZ 86011, USA.

*Author for correspondence (triede@midwestern.edu)

T.R., 0000-0001-6875-0017

Received 21 February 2020; Accepted 7 May 2020

Journal of Experimental Biology (2020) 223, jeb223925. doi:10.1242/jeb.223925

pygmy mice is described as a 'high-pitched, barely audible squeal' produced with the head 'thrust forward and upward, stretching the throat' (Blair, 1941). Miller and Engstrom (2007) reported that songs were produced by both sexes and were not as elaborate as those produced by sister taxa neotropical singing mice (*Scotinomys*; Pasch et al., 2011, 2013). How such frequency-modulated songs are produced is unknown but promises to provide important insight into the evolution of signal elaboration in the largest radiation of mammals.

In this study, we used acoustic recordings in normal air and a light gas mixture to determine the mode of vocal production of northern pygmy mouse songs. The use of gases that are lighter or heavier than ambient air has a long tradition in the study of vocal production mechanisms (e.g. Beil, 1962; Nowicki, 1987; Pasch et al., 2017). Sounds produced via a whistle mechanism demonstrate a characteristic increase in fundamental frequency in helium atmosphere that is distinct from the constancy of fundamental frequencies produced via flow-induced vocal fold vibration (Spencer and Titze, 2001). We then used contrast-enhanced micro-computed tomography (CT) imaging and histology to characterize the laryngeal anatomy subserving such unique sound production. Finally, we used geometric morphometrics to compare laryngeal differences within pygmy mice and among closely related species to assess the contribution of larynx and ventral pouch size and shape to acoustic diversity.

MATERIALS AND METHODS

Animals

We captured northern pygmy mice, *Baiomys taylori* (Thomas 1887), near Rodeo, NM, USA, using Sherman live-traps baited with sterilized bird seed. Mice were transferred in standard mouse cages to animal facilities at Northern Arizona University, Flagstaff, AZ, USA, maintained on a 14 h light:10 h dark cycle (21±2°C) and provided with rodent chow, bird seed and water *ad libitum*. A subset of animals was transferred to Midwestern University, Glendale, AZ, USA, for heliox experiments and morphological analysis. All procedures in studies involving animals were performed in accordance with the ethical standards and approval of the Institutional Animal Care and Use Committee at Midwestern University (MWU#2852) and Northern Arizona University (16-001 and 19-006) and guidelines of the American Society of Mammalogists (Sikes et al., 2016). Animals were captured with permits from the New Mexico Department of Game and Fish (3562) and the Arizona Game and Fish Department (607608).

Acoustic recording, heliox experiments and statistical analyses

We recorded the mass and vocalizations of 10 wild-captured mice (n=5 per sex) over 10 days. Singly housed mice in their home cage were placed in semi-anechoic coolers lined with acoustic foam. We used 1/4 inch microphones (Type 40BE, G.R.A.S.) connected to preamplifiers (Type 26 CB, G.R.A.S.) to obtain recordings 33.3 cm above the center of the focal mouse cage. Microphone response was flat within ±1.5 dB from 10 Hz to 50 kHz, and pre-amplifier response was flat within ±0.2 dB from 2 Hz to 200 kHz. Microphones were connected to a National Instruments DAQ (USB 4431) sampling at 102.4 kHz and to a desktop computer running MATLAB (version 2018a).

We used Avisoft SASLab Pro [version 5.2.13, Avisoft Bioacoustics; 1024-point Fast Fourier Transform (FFT), 75% frame size, Hann window, frequency resolution 100 Hz, temporal resolution 93.75%, 0.625 ms] to automatically extract temporal (song duration) and spectral [maximum and minimum fundamental frequency (F_0), and frequency bandwidth averaged across all notes in the song] parameters from each bandpass-filtered (17.5–40.5 kHz) recording.

Student's t-tests were used to compare body mass, number of songs and acoustic parameters between females and males in JMP Pro (version 14.1.0, SAS Institute, Inc., Cary, NC, USA). We used a Bonferroni correction to control for multiple (n=5) comparisons (corrected α=0.01). We also assessed whether repeatability of acoustic parameters differed between the sexes by calculating intraclass correlation coefficients (ICC; Wolak et al., 2012) using the ICC R package (version 2.3.0; Wolak et al., 2012) in R version 3.6.1 (http://www.R-project.org/). Acoustic parameters were considered repeatable if the 95% confidence interval (CI) of ICC values excluded zero, and similar between sexes if CIs overlapped one another. Values are reported as means±s.d. in the text.

Songs of six additional animals (3 songs per sex per treatment) were recorded in normal air and in a heliox atmosphere. Individual mice were placed in a standard mouse cage. The cage was equipped with bedding, food and water. Heliox gas (80% He, 20% O_2) was injected into the cage at flow rates between 20 and 40 l min^{-1} through a 12 mm wide tube placed into the cage wall near the floor. Predicted effects of light gas concentrations were estimated with a small whistle placed at the floor of the cage and connected externally by a silastic tube. The whistle was blown and recorded at regular intervals in order to monitor the heliox concentration. The ratio of the frequency of the whistle in air and in heliox allowed an estimation of the expected effect for any given heliox concentration.

Three randomly selected syllables (from the first, second and last third of the song) from each song were analyzed for minimum and maximum F_0, syllable duration, and relative amplitude of the first and second harmonic of the F_0. While conducting the experiments, we noticed that the temporal characteristics of songs changed in heliox. Therefore, we measured syllable repetition rate, syllable duration and intersyllable interval (i.e. the duration between two adjacent syllables) for three songs in normal air and three in heliox. Syllable repetition rate was calculated by dividing the number of syllables within a song by song duration. Syllable duration and intersyllable interval were averaged over all syllables of a song. Acoustic differences between normal air and heliox songs were assessed with paired t-tests.

Histology, CT scanning and 3D rendition of the larynx

Ten mice (5 per sex) were euthanized with isoflurane and then transcardially perfused with saline solution followed by 10% buffered formalin. Larynges were dissected and placed in 10% buffered formalin phosphate (SF100-4; Fisher Scientific) for 2 days.

Four specimens (2 per sex) were used to prepare histological sections. Mid-membraneous coronal sections (5 mm thick) were stained with hematoxylin–eosin for a general overview. We also attempted to use Masson's Trichrome (TRI) for collagen fiber stain and Elastica van Gieson (EVG) for elastic fiber stain. However, pygmy mouse vocal folds are small (see below), and we were unsuccessful in collecting a sufficient sample size of mid-membraneous sections for different stains in each individual. Sections were scanned with an Aperio CS 2 slide scanner and processed with Imagescope software (version 8.2.5.1263; Aperio Tech.).

Two specimens (1 per sex) were whole-body scanned at 50 µm resolution. Larynges from these two individuals and four additional mice (3 per sex) were also X-rayed at 5 µm resolution. First, tissues were transferred from the formalin solution to 99% ethanol. Tissues were then stained in 1% phosphotungstic acid (PTA; Sigma-

Journal of Experimental Biology (2020) 223, jeb223925. doi:10.1242/jeb.223925

Aldrich, 79690) in 70% ethanol. After 5 days, the staining solution was renewed and the tissue was stained for another 5 days. After staining, specimens were placed in a custom-made acrylic tube and scanned in air. CT scanning was done using a Skyscan 1172 (Bruker). Reconstructed image stacks were then imported into AVIZO software (version Lite 9.0.1). Laryngeal cartilages and the border between the airway and soft tissues of the larynx in the CT scans were traced manually. This approach provided outlines of the cartilaginous framework and the airway. Derived 3D surfaces of all six specimens have been archived at Morphobank (http://www.morphobank.org, project # 3638).

Geometric morphometric analysis of laryngeal shape

We investigated whether the laryngeal size or shape of *B. taylori* mice was sexually dimorphic using a geometric morphometric (GM) approach. 3D surfaces of three male and three female laryngeal cartilages were used to quantify shape using curve and surface landmarks. Landmarks were placed on surface renderings using the 'geomorph' package, version 3.0.5 (https://cran.r-project.org/package=geomorph) for the R software package (http://www.R-project.org/). Fixed landmarks were placed along the cartilage border and supplemented by 100 surface semi-landmarks, which were placed with the help of an interactive function to build a template of 3D surface semi-landmarks. In order to compare cartilage shape, a generalized Procrustes analysis was used to remove variation related to position, size and orientation. Next, we employed a series of principal components analyses (PCA) to summarize the main patterns of shape variance in the data. The procedure used here has been previously established (Borgard et al., 2019).

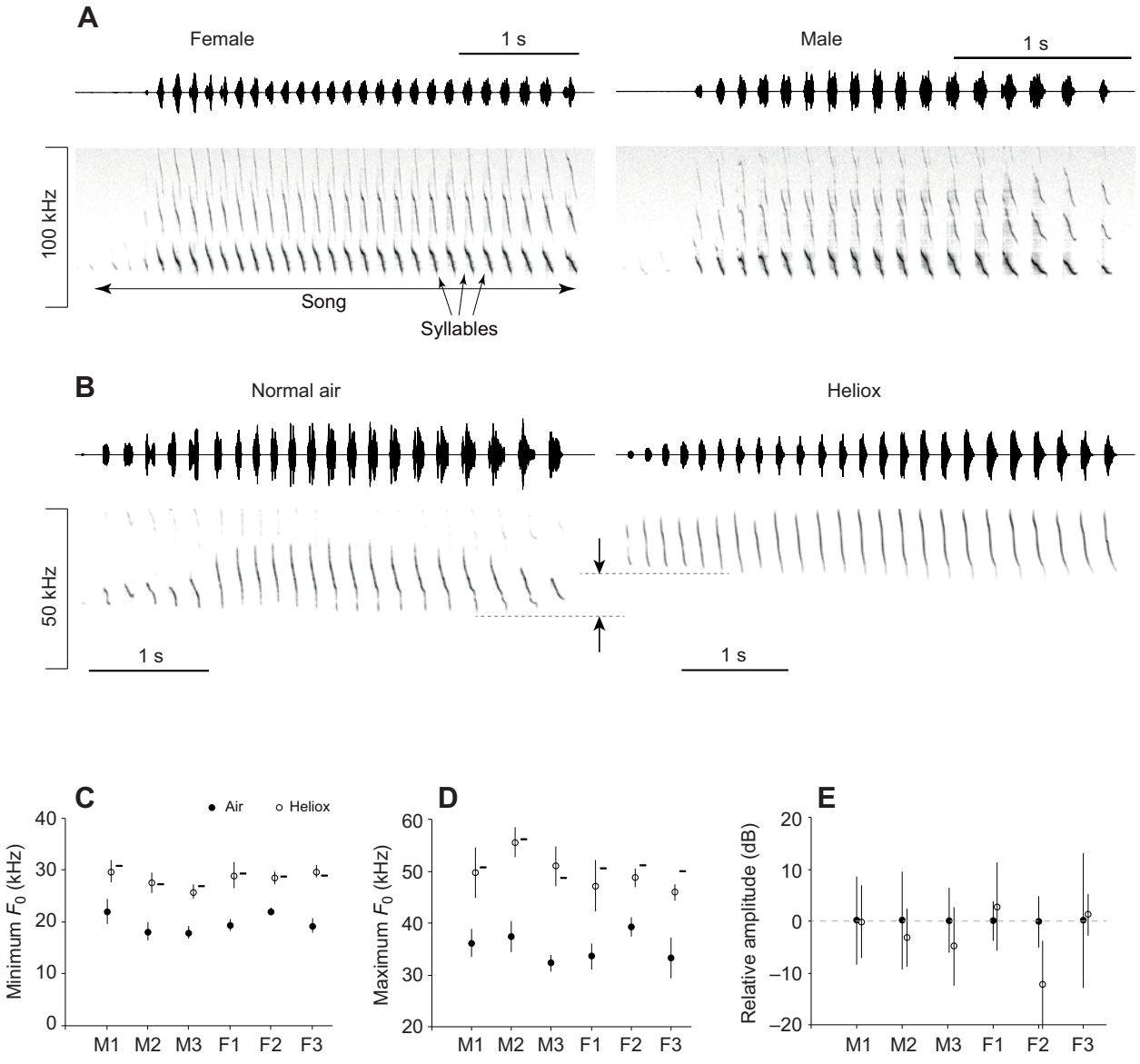

Fig. 1. Baseline acoustic recordings. (A) Representative spectrograms of a female and a male northern pygmy mouse (*Baiomys taylori*) long-distance vocalization (song). The song consists of multiple frequency-modulated syllables. (B) Representative songs of a pygmy mouse in air and in a helium–oxygen mixture (heliox). Note the increase in fundamental frequency (F_0) in heliox (the frequency scale is different from that in A). (C) Minimum F_0 for 6 animals in air and in heliox. (D) Maximum F_0 for 6 animals in air and in heliox. Horizontal bars in C and D indicate the expected increase of F_0 in heliox. (E) Relative amplitude (ratio of $2F_0/F_0$) for three songs in 3 females (F1–F3) and 3 males (M1–M3). Data in C–E are means±s.d.

Journal of Experimental Biology (2020) 223, jeb223925. doi:10.1242/jeb.223925

Table 1. Mean±s.d. parameters and repeatability estimates for female and male northern pygmy mice (*Baiomys taylori*) vocalizations

Parameter	Female	Male	d.f.	*t*	*P*	Repeatability (95% CI) (all, females, males)
Body mass (g)	9.95±1.1	9.22±0.8	8	−1.23	0.25	–
Number of songs	53±52.3	162.8±134.6	8	1.69	0.13	–
Duration (s)	3.4±0.4	4.9±0.5	8	4.99	**0.001**	0.37 (0.21–0.66) 0.19 (0.06–0.68) 0.13 (0.05–0.56)
Maximum F_0 (kHz)	33.8±2.2	33.1±1.3	8	−0.68	0.52	0.63 (0.44–0.85) 0.77 (0.54–0.97) 0.61 (0.36–0.93)
Minimum F_0 (kHz)	23.5±1.9	21.0±1.0	8	−2.51	0.046	0.63 (0.44–0.85) 0.66 (0.4–0.94) 0.44 (0.22–0.87)
F_0 bandwidth (kHz)	10.4±0.5	12.1±1.3	8	2.58	0.048	0.65 (0.47–0.86) 0.1 (0.03–0.53) 0.59 (0.33–0.92)

F_0, fundamental frequency; CI, confidence interval. Bold *P*-values reflect significance following a Bonferroni correction for multiple comparisons. n=5 per sex.

Centroid size was used to estimate overall size for each cartilage. Centroid size is the square root of the sum of squared distances of each landmark from the center of the cartilage. The location is obtained by averaging the x, y and z coordinates of all landmarks (Zelditch et al., 2004).

For comparative analyses, we used data from laboratory mice (*Mus musculus*), laboratory rats (*Rattus rattus*) and grasshopper mice (*Onychomys* spp.) published previously by Borgard et al. (2019). To assess whether laryngeal cartilage shape exhibited sex differences in pygmy mice, we performed a multivariate analysis of variance (MANOVA) on the PC1 and PC2 scores for each cartilage.

RESULTS

Baseline acoustic recording

Long-distance songs consisted of repeated frequency-modulated syllables (Fig. 1A). All song parameters were repeatable within individuals and between sexes (Table 1). We found no sex differences in mass (females: 9.95±1.1 g; males: 9.22±0.8 g; t_8=−1.23, P=0.25) nor number of songs produced (females: 53±52.3 songs; males: 162.8±134.6 songs; t_8=1.69, P=0.13; Table 1) despite males showing higher variation in song rate (range: 84–401 songs) than females (range: 5–132 songs). Males produced longer songs with slightly lower minimum F_0 and larger frequency bandwidths compared with females (Table 1).

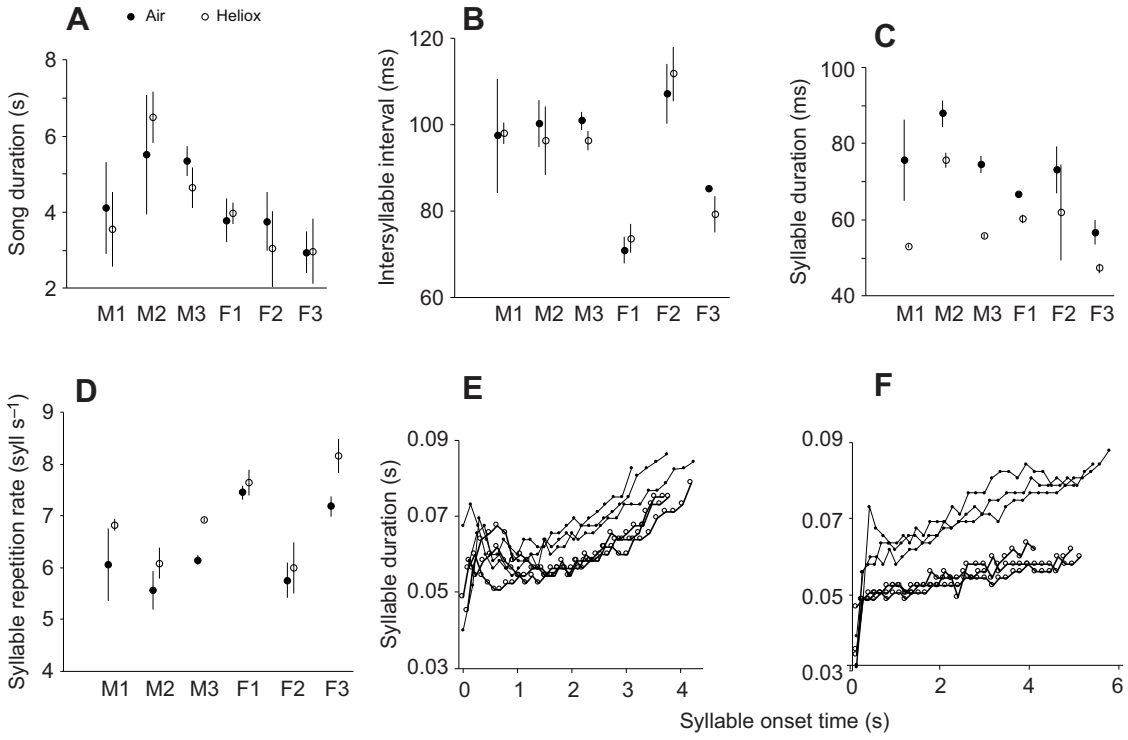

Fig. 2. Temporal features of song in air and heliox. (A) Song duration, (B) intersyllable interval, (C) syllable duration and (D) syllable repetition rate over the entire song. Data are means±s.d. Syllable duration was consistently shorter in heliox. (E,F) Syllable duration across three songs in air and three in heliox for a female (E) and a male (F) mouse.

Journal of Experimental Biology (2020) 223, jeb223925. doi:10.1242/jeb.223925

Heliox experiments

Both maximum and minimum F_0 increased in heliox (paired *t*-test, maximum F_0: $t=-10.0$, $P<0.001$; minimum F_0: $t=-14.1$, $P<0.001$) compared with those in normal air (Fig. 1B–D). However, the amplitude of higher harmonics ($2F_0$) in normal air and in heliox relative to F_0 at the center of syllables did not differ (paired *t*-test, $t=-1.3$, $P=0.261$; Fig. 1E).

While song duration and intersyllable interval did not differ between normal air and heliox (paired *t*-test, song duration: $t=0.70$, $P=0.513$; intersyllable interval: $t=0.61$, $P=0.566$; Fig. 2A,B), other temporal features of the song changed in heliox. Syllable duration decreased significantly (paired *t*-test, $t=5.5$, $P<0.01$) and, as intersyllable interval was unaltered, syllable repetition rate increased (paired *t*-test, $t=-4.6$, $P<0.01$) (Fig. 2C,D). Fig. 2E,F shows individual syllable durations over the course of three songs in normal air and in heliox, for a male and a female mouse. Syllable duration decreased by 15±6.7% and syllable repetition rate increased 10.5±4.4%, yet the number of syllables per song did not change significantly (number of syllables in air: 28.9±4.6, in heliox: 29.5±6.9; $t=0.88$, $P=0.422$; Table 1).

Pygmy mouse vocal apparatus morphology

The membraneous portion of a vocal fold (captured by six sequential sections in Fig. 3A–F) refers to the soft tissue that starts at the vocal process of the arytenoid cartilage and ends where the vocal fold attaches to the interior of the thyroid cartilage. The ventral section of the membraneous portion of the vocal fold is reinforced with cartilaginous tissue and is continuous with the alar cartilage and epiglottis. Consequently, the cartilaginous-free, membraneous portion of the vocal fold is very short (<150± 24 µm; $n=4$). The membraneous portion of the vocal fold is composed of thyroarytenoid muscle, lamina propria and epithelium. The lamina propria of the membraneous portion is composed of a thick layer (up to 110±1.5 µm) of collagen and elastic fibers (Fig. 3G).

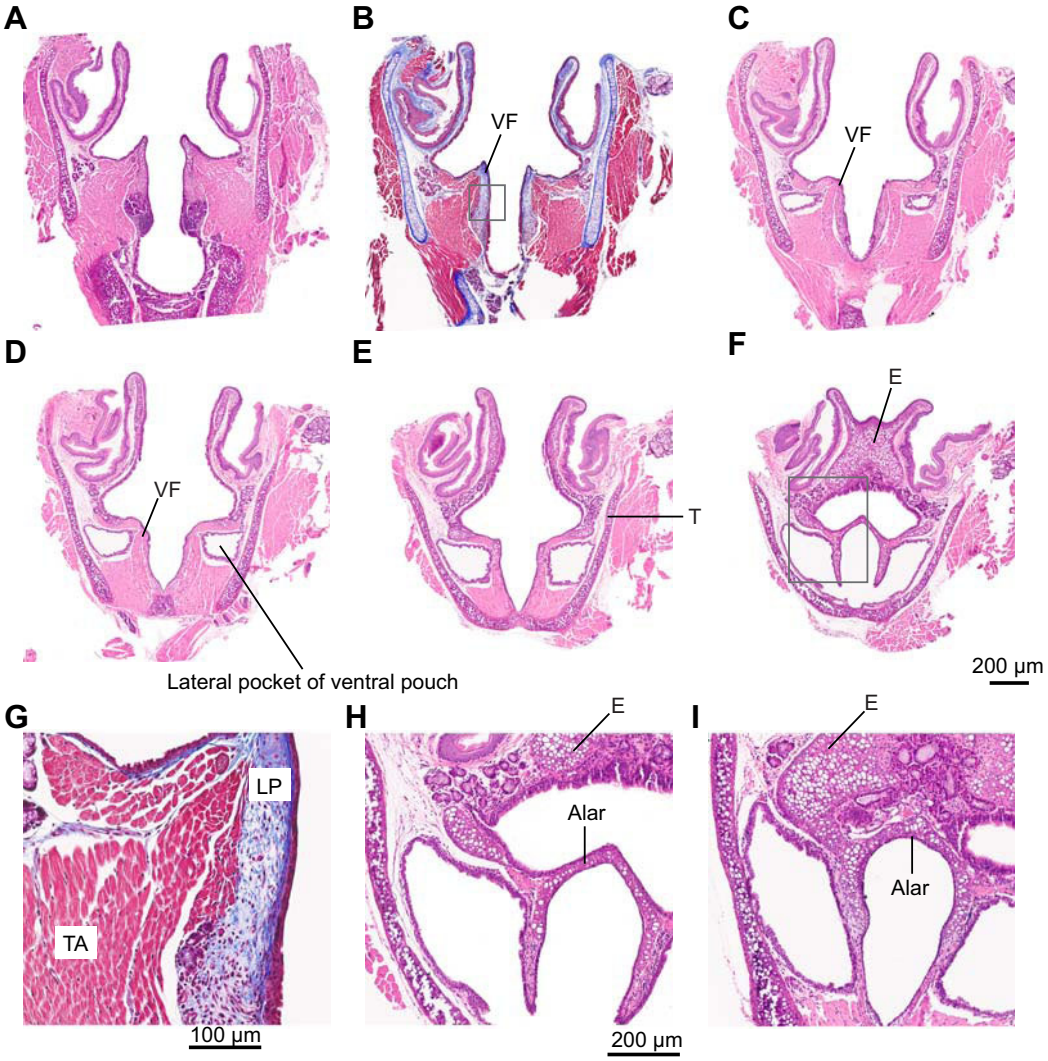

Fig. 3. Coronal serial sections through the larynx of a male pygmy mouse. (A–F) Dorsal to ventral sections, 50 µm apart. In B, there is still part of the arytenoid cartilage present in the vocal fold. The membraneous portion of the vocal fold (i.e. no cartilage present) is shown in D and E. In F, cartilage is present, which is part of the alar cartilage. The lateral pocket of the ventral pouch is visible in C–F. The boxed regions in B and F are magnified in G and H, respectively. (I) Image taken from a section subsequent to F showing that the cartilage in the vocal fold is part of the alar cartilage, and that the alar cartilage is connected to the epiglottis. Scale bar in F applies to A–F. Scale bar in H applies to H and I. E, epiglottis; T, thyroid cartilage; VF, vocal fold; TA, thyroarytenoid muscle; LP, lamina propria of the vocal fold.

Journal of Experimental Biology (2020) 223, jeb223925. doi:10.1242/jeb.223925

The ventral pouch of *B. taylori* is large with a medially positioned portion rostral from the vocal folds (Fig. 4A). Additionally, pockets connected to the medial portion extend laterally from each vocal fold, causing a unique morphology of the ventral portion of the vocal fold unprecedented in the mammalian larynx (e.g. Negus, 1949; Schneider, 1964). The vocal fold is very thin and membranous (Fig. 3C–F). The alar cartilage forms the edge of the entrance into the ventral pouch. Fig. 3H,I shows representative images of the cartilage. Histological sections demonstrate that the cartilage is associated with the epiglottis (Fig. 3I).

The thyroid cartilage consists of a left and right lamina, each with a rostral and caudal horn (Fig. 5A–D). The rostral horn is narrow and pointed. The rostro-ventral margin of the thyroid bends dorsally, toward the laryngeal lumen forming a bulla thyroidea (Fig. 5D). The ventral pouch is embedded in this bulla. A small cartilaginous protuberance is present on the medial surface of the thyroid cartilage in a caudal midsagittal position (Fig. 5B). The structure consists of highly mineralized cartilage that protrudes into the laryngeal lumen. Vocal folds attach to the thyroid cartilage via this protuberance.

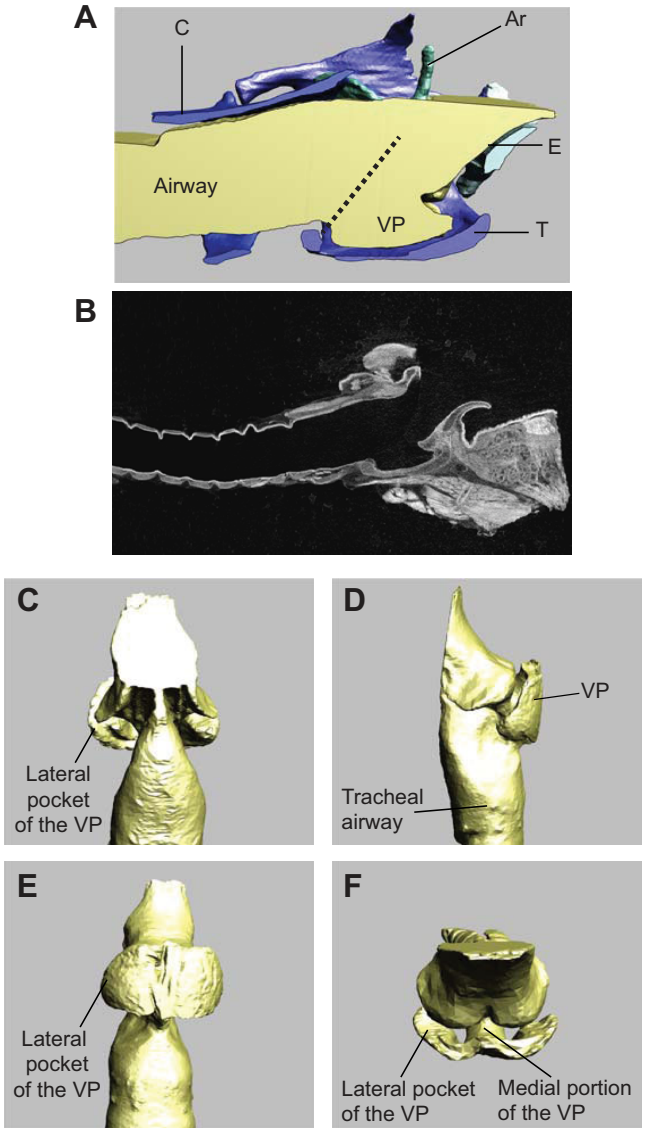

Fig. 4. Vocal apparatus morphology. (A) Lateral view of a midsagittal section through the 3D reconstruction of laryngeal cartilages and laryngeal airway of a male pygmy mouse. The dashed line indicates the position of the cranial edge of the vocal fold. (B) CT image of a midsagittal view of a female pygmy mouse larynx. (C–E) 3D surface rendition of the airway in four different views: dorsal (C), right lateral (D), ventral (E) and top (F). Ar, arytenoid cartilage; E, epiglottis; T, thyroid cartilage; VP, ventral pouch; C, cricoid cartilage.

The cricoid cartilage (Fig. 5E–H) forms a complete ring with a broad plate dorsally and a narrow band laterally and ventrally. The arytenoid cartilages form triangular shaped structures with a vocal process, a short muscular process and a long and narrow dorsal process (aka apex) (Fig. 5I–L). The epiglottis (Fig. 5M–P) forms a small sheet bending towards the airway. Most notable is the structure at the caudal end of the epiglottis, which is described as alar cartilage in other species. In *M. musculus*, *R. rattus* and *Onychomys* spp., the alar cartilage was a separate structure without connection to another laryngeal cartilage (Riede et al., 2017). In *B. taylori*, the alar cartilage supports the entrance into the ventral pouch and is moved by fibers from the thyroarytenoid muscle. Unlike in *M. musculus*, *R. rattus* and *Onychomys* spp., the alar cartilage is tightly connected with the epiglottis in *B. taylori*.

The length of the oral and pharyngeal cavity (vocal tract length measured between the vocal fold and tip of incisivi) measured 16 and 17 mm in a female and male specimen, respectively, for which the whole body was scanned before the larynx was excised for high-resolution scanning.

Analysis of larynx size and shape

Laryngeal size represents an important source of spectral differences in animal vocalizations. We therefore investigated the size and shape of laryngeal cartilages as well as the ventral pouch. First, we tested for morphological differences between sexes in *B. taylori*, and then compared larynx size of *B. taylori* with that of *M. musculus*, *R. rattus* and *Onychomys* spp. in order to explain the fundamental frequency of *B. taylori* songs.

Neither the size of the four laryngeal cartilages nor any of the ventral pouch dimensions demonstrated sexual dimorphism in *B. taylori* (Table 2). Cartilage shape was also not different between the sexes. None of the four cartilages exhibited separation of their shape along the first or second principal component (PC1 and PC2) (thyroid cartilage: $F_{1,3}$=0.88, P=0.21; Wilks' Λ=0.82; cricoid cartilage: $F_{1,3}$=0.89, P=0.21; Wilks' Λ=0.82; arytenoid cartilage: $F_{1,3}$=0.85, P=26; Wilks' Λ=0.78; epiglottis: $F_{1,3}$=0.64, P=0.84; Wilks' Λ=0.51) (Fig. 6A–D).

Compared with three other species, *B. taylori* possesses a very large and unusually shaped ventral pouch (Fig. 7A–D). Overall larynx size remains linked to body size (Fig. 7E–H). All four cartilages scaled with negative allometry against body mass. Interestingly, the size of the ventral pouch, a structure which is located inside the larynx, is not linked to larynx size or body size (Fig. 7I–J). However, ventral pouch dimensions, in particular its latero-lateral width, appear to be associated with F_0 among the four species (Fig. 7K, Table 3).

DISCUSSION

Our findings indicate that the elaborate singing behavior of baiomyine mice arises from a unique laryngeal morphology that facilitates aerodynamic whistle production. In particular, a large air sac termed the ventral pouch and a robust alar cartilage are associated with the production of F_0 through an aerodynamic whistle. In rodents, the presence of a ventral pouch and alar cartilage are associated with ultrasonic whistle production, and damage to the alar cartilage and

Journal of Experimental Biology (2020) 223, jeb223925. doi:10.1242/jeb.223925

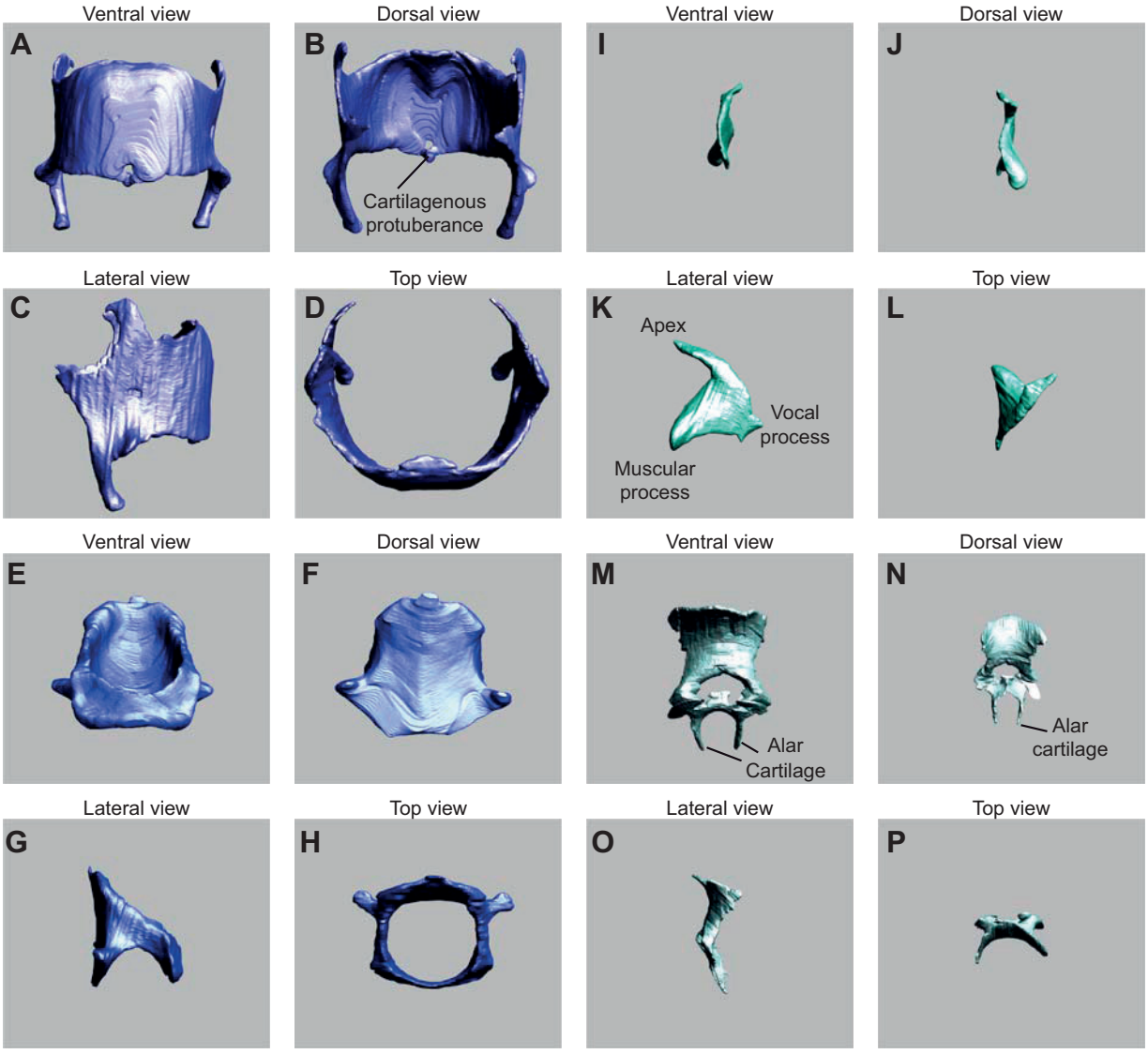

Fig. 5. 3D surface renditions of laryngeal cartilages of a male northern pygmy mouse. (A–D) Thyroid cartilage. (E–H) Cricoid cartilage. (I–L) Arytenoid cartilage. (M–P) Epiglottis.

ventral pouch compromises whistle fidelity (Riede et al., 2017). Our current findings further support the association between the presence of a ventral pouch and alar cartilage and the ability to produce ultrasonic vocalizations by an aerodynamic whistle mechanism. More specifically, comparative analyses indicate that ventral pouch size is associated with F_0, allowing relatively small species to produce low-frequency songs independent of body size (Table 3). Our findings provide important insight into the anatomical innovations that facilitate signal elaboration.

The relatively low F_0 of pygmy mouse songs are remarkable because they are among the smallest rodents (8–12 g; Wilson and Reeder, 2005). The songs extend to the lowest aerodynamic whistle frequency recorded among four species for which anatomical information and light gas experiments have informed our understanding of the vocal production mechanisms. From one perspective, pygmy mouse ultrasonic whistles overlap the audible calls of grasshopper mice, a genus that is larger in mass (32–38 g) and produces long-distance vocalizations using vocal fold vibrations (Pasch et al., 2017). Conversely, pygmy mouse frequencies also overlap with the lowest ultrasonic frequencies reported for laboratory rats (19 kHz; Brudzynski et al., 1993; Wright et al., 2010), which are 10–20 times larger than pygmy mice (250–500 g; Wilson and Reeder, 2005). In addition, pygmy mouse song frequencies are much lower than those of laboratory mouse (*M. musculus*) songs (Holy and Guo, 2005), a species that is slightly larger (25–50 g; Wilson and Reeder, 2005), but whose ventral

Table 2. Mean±s.d. parameters for female and male northern pygmy mice (*B. taylori*) laryngeal cartilage size

Parameter	Female	Male	d.f.	*F*	*P*
$\log_{10}$(CS thyroid cartilage)	4.03±0.01	4.03±0.01	1, 6	0.17	0.70
$\log_{10}$(CS cricoid cartilage)	3.85±0.01	3.85±0.01	1, 6	0.01	0.99
$\log_{10}$(CS arytenoid cartilage)	3.43±0.03	3.42±0.01	1, 6	0.09	0.93
$\log_{10}$(CS epiglottis)	3.49±0.03	3.43±0.04	1, 6	3.7	0.13
Ventral pouch LL (mm)	963±116	935±38	1, 6	0.15	0.71
Ventral pouch VD (mm)	355±71	386±28	1, 6	0.50	0.52
Ventral pouch CC (mm)	876±38	856±95	1, 6	0.11	0.75
Ventral pouch A1 (mm)	568±164	550±173	1, 6	0.18	0.90

CS, centroid size; LL, latero-lateral; VD, ventro-dorsal; CC, cranio-caudal; A1, distance between glottis and alar edge of ventral pouch entrance. *n*=3 per sex.

Journal of Experimental Biology (2020) 223, jeb223925. doi:10.1242/jeb.223925

Table 3. Pearson correlation coefficients for three spectral parameters and body mass, laryngeal size and ventral pouch size

	Minimum F_0	Maximum F_0	Mean F_0
$\log_{10}$(body mass)	R=−0.33, P=0.67	R=0.40, P=0.60	R=0.28, P=0.72
$\log_{10}$(CS thyroid)	R=−0.29, P=0.71	R=0.41, P=0.59	R=0.29, P=0.71
$\log_{10}$(CS cricoid)	R=−0.29, P=0.71	R=0.44, P=0.56	R=0.32, P=0.68
$\log_{10}$(CS arytenoid)	R=−0.24, P=0.75	R=0.49, P=0.51	R=0.37, P=0.63
$\log_{10}$(CS epiglottis)	R=0.29, P=0.71	R=0.73, P=0.27	R=0.67, P=0.33
VP-LL	***R*=−0.87, *P*=0.13**	R=−0.52, P=0.48	R=−0.61, P=0.39
VP-DV	R=−0.42, P=0.58	R=0.20, P=0.79	R=0.09, P=0.91
VP-CC	R=−0.54, P=0.46	R=0.15, P=0.85	R=0.02, P=0.98
VP-A1	R=−0.07, P=0.97	R=0.64, P=0.36	R=0.54, P=0.46

The correlation between the latero-lateral (LL) dimension of the ventral pouch and minimal fundamental frequency (F_0) reached the greatest association.

pouch is much smaller than that of *Baiomys* (Riede et al., 2017; herein). Thus, while the overall size of the vocal apparatus appears to scale linearly with body size (Fig. 7E–H), the dimensions of the ventral pouch uncouple the relationship between body size and size-dependent acoustic features (Fig. 7I–K).

The fundamental frequency of USVs depends on glottal airflow velocity, the distance between the glottal and alar edge, and ventral pouch volume (Riede et al., 2017). Our data suggest that laryngeal cartilage size scaled allometrically with body size but was not associated with vocal frequencies. In contrast, ventral pouch size was inversely related to maximum and minimum F_0 across species and likely explains the low frequency range of *Baiomys* songs. While the ventral pouch did not explain sexual dimorphism of acoustic features in the songs of pygmy mice, the slight difference (2 kHz) in spectral content between the sexes may be too minimal to detect with our methodology. Alternatively, sex differences in muscle tension may contribute to laryngeal shape and size differences that mediate vocal output (Riede, 2013).

Air sacs, ventricles, bullae and ventral pouches

Side branches or cavities branching off the main upper airway above and below the laryngeal valve are common in mammals and birds (e.g. King and McLelland, 1984; Riede et al., 2008). Such rigid or inflatable cavities serve to amplify sound levels, modify existing resonance properties or introduce an additional resonance frequency (Riede et al., 2008; deBoer, 2009). In rodents, the air sac or ventral pouch is different from air sacs in non-human primates, cervids and birds. Whereas non-rodent air sacs can branch off the airway above or below the glottis, the rodent ventral pouch is always positioned rostral to the glottis, embedded inside the thyroid cartilage lumen and supported by cartilaginous structures. The alar cartilage or modifications of the epiglottis reinforce the entrance and lateral wall of the ventral pouch. Riede et al. (2017) suggested that the alar edge of the reinforced entrance acts like the blade or labium of the air hole of a recorder. The glottal airflow is guided over the ventral pouch entrance and hits the alar edge which opposes the glottis, generating pressure fluctuations that presumably excite resonances inside the ventral pouch. In addition, the alar cartilage is associated with a

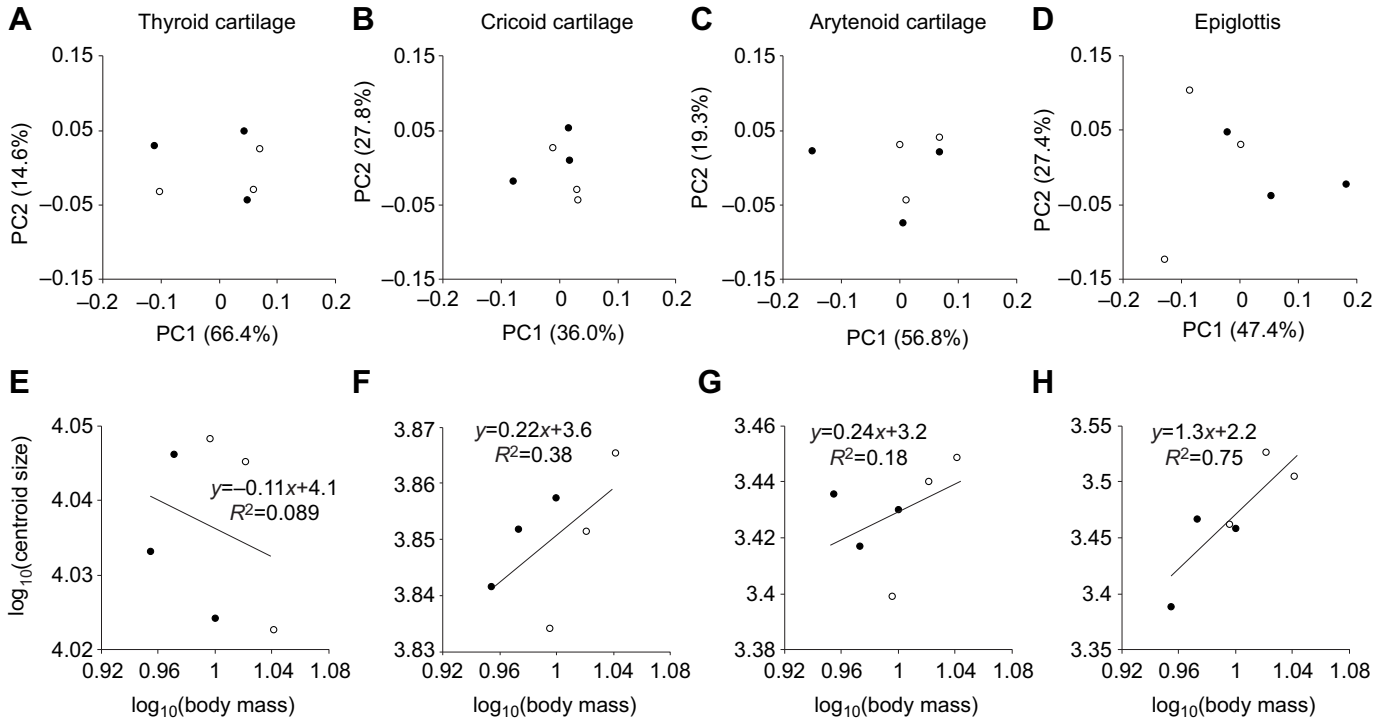

Fig. 6. Analysis of larynx size and shape. (A–D) Principal component analysis of the Procrustes shape coordinates from curve and surface semi-landmarks for thyroid (A), cricoid (B), arytenoid (C) cartilage and epiglottis (D). Each point represents the cartilage shape of one individual (filled circles, males; open circles, females). (E–H) Relationship between cartilage size (measured as centroid size) and body mass for thyroid (E), cricoid (F), arytenoid (G) cartilage and epiglottis (H).

Journal of Experimental Biology (2020) 223, jeb223925. doi:10.1242/jeb.223925

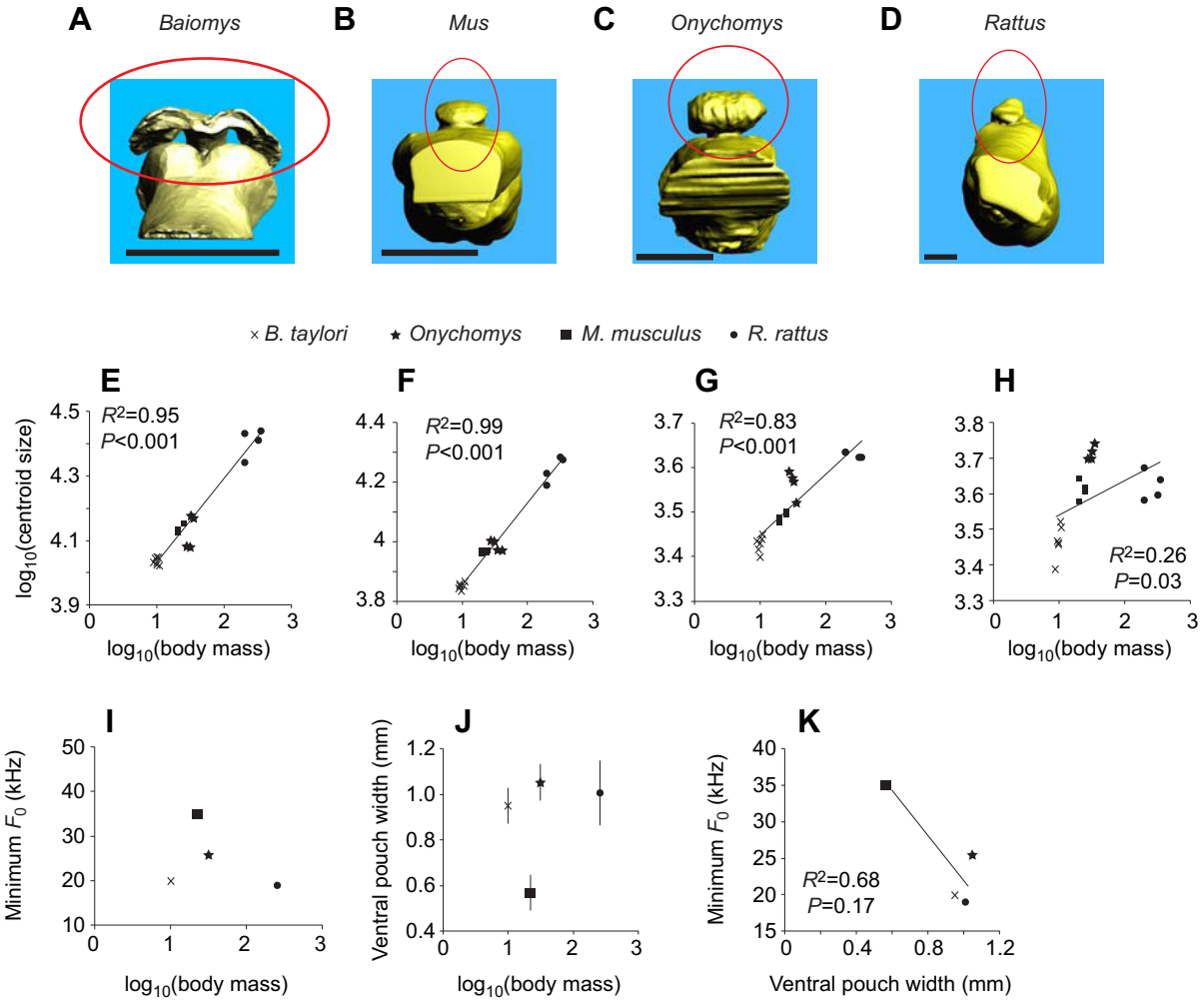

Fig. 7. *Baiomys taylori* possesses large ventral pouch. (A–D) Cranio-caudal views of the ventral pouch of four rodent species that produce ultrasonic whistles: *B. taylori* (A), *M. musculus* (B), *Onychomys* spp. (C) and *R. rattus* (D). Scale bars: 1 mm. (E–H) Relationships between body mass and centroid size of thyroid (E), cricoid (F) and arytendoid (G) cartilage and epiglottis (H). (I–K) Relationships between minimum F_0 of ultrasonic vocalizations and body mass (I), between body mass and ventral pouch size (latero-lateral dimension; J) and between ventral pouch size and minimum F_0 (K).

small body of muscle fibers branching off from the thyroarytenoid muscle, and activity of this muscle is precisely associated with F_0 features of vocalizations (Riede, 2013). Together, our anatomical findings suggest that the dimensions of the rodent ventral pouch, unlike those of other air sacs, are precisely controlled.

Vocal–respiratory coordination

Most heliox studies in bioacoustics focus on spectral analysis because resultant patterns are indicative of underlying production mechanisms. We hypothesize that heliox experiments can also inform our understanding of vocal–respiratory coordination. In particular, we found that pygmy mouse syllables were shorter in duration in heliox than in air. Our findings are in accordance with heliox-induced shortening of vocalizations in grasshopper mice (*Onychomys*; Pasch et al., 2017) and common marmosets (*Callithrix jacchus*; Zhang and Ghazanfar, 2018) that both produce vocalizations by airflow-induced vocal fold vibration. The magnitude of the effect was similar among species (*B. taylori*, 15%; *Onychomys*, 19%; *C. jacchus*, 11%). We speculate that the lower density of inhaled heliox affects laryngeal aerodynamics by an eased gas flow through the constricted glottal valve during vocal production (Sundberg, 1981). Consequently, a slightly reduced air volume is available during expiration to decrease syllable duration. Confirmation of this hypothesis will require further experimentation with varying concentrations of light gas and/or use of heavy gas.

Our findings provide further insight into vocal–respiratory coordination when contextualized in relation to recent work in another baiomyine rodent (Alston's singing mouse; *Scotinomys teguina*) that produces a similar repetitive song (e.g. Campbell et al., 2010; Pasch et al., 2011). Okobi et al. (2019) found that cooling of the orofacial motor cortex decreased the rate of change of syllable duration without affecting the duration of individual syllables. While not explicitly stated, cooling appears to do so by increasing the duration of the inhalation phase (i.e. intersyllable interval), which directly contrasts our heliox findings, which show an impact on the expiratory phase (syllable duration) without changing intersyllable interval. Together, available data suggest that songs emerge from a motor pattern coded by a central pattern generator in the brainstem (Tschida et al., 2019) whose timing is modulated by cortical control of breathing (specifically the inhalation phase) (Okobi et al., 2019). Differences in the acoustic output, however, can also simply be the result of mechanical constraints of the peripheral organ; for example, laryngeal aerodynamics that are sensitive to airflow (this study). Integration of laryngeal and

breathing movements coupled with a detailed understanding of vocal organ morphology and laryngeal aerodynamics provides a fuller understanding of the nature of rodent acoustic signals and their evolution.

Conclusions

Ultimately, understanding how acoustic characters evolve requires knowledge of how signals are produced. Our findings indicate that diversity in the size of a unique laryngeal structure termed the vocal pouch is associated with extreme divergence in F_0 of ultrasonic whistles. Thus, the traditional approach of categorizing vocal signals by spectral range into 'audible' (up to 16 kHz) and 'ultrasonic' (above 19 kHz) vocalizations requires revision. Indeed, the challenge of differentiating 'audible' and 'ultrasonic' vocalizations in rodents has been noted (e.g. Grimsley et al., 2016; Kalcounis-Rueppell, 2010, 2018; Miller and Engstrom, 2007, 2010, 2012). A production-based definition that distinguishes between flow-induced vocal fold vibration and aerodynamic whistles provides a more robust framework to explore diversification of rodent voices. Heliox experiments confirmed that the ultrasonic songs in pygmy mice are aerodynamic whistles and can reach low into the 'sonic' frequency range. Other species may have adaptations that extend the spectral range of whistles to low frequencies (this study) or the range of flow-induced vocal fold vibrations into exceptionally high spectral regions (e.g. Titze et al., 2016). The present study also informs our understanding of the vocal production mechanism, which requires precise coordination between three systems (larynx, breathing and vocal tract). Aerodynamics at the vocal folds (vibrating or not) are determined not only by the coordination of the three systems but also by the laryngeal morphology and biomechanical properties.

Altogether, the current study demonstrates that rodents are a promising system for understanding how mechanisms of complex behaviors like vocal production may promote or constrain divergence.

Acknowledgements

We thank Nathaniel Mull for assistance in trapping animals in the field and Bryan Carlin for assistance with recording animals in the laboratory.

Competing interests

The authors declare no competing or financial interests.

Author contributions

Conceptualization: T.R., B.P.; Methodology: T.R., B.P.; Formal analysis: T.R., B.P.; Data curation: T.R., B.P.; Writing - original draft: T.R., B.P.; Writing - review & editing: T.R., B.P.; Funding acquisition: T.R., B.P.

Funding

This study was funded by the National Science Foundation [IOS 1755429 to B.P. and IOS 1754332 to T.R.].

Data availability

Derived 3D surfaces have been archived at Morphobank, project 3638: http://morphobank.org/permalink/?P3638

References

Bailey, V. (1931). Mammals of New Mexico. *N. Am. Fauna* **53**, 422. doi:10.5962/bhl.title.86644

Beil, R. G. (1962). Frequency analysis of vowels produced in a helium-rich atmosphere. *J. Acoust. Soc. Am.* **34**, 347-349. doi:10.1121/1.1928124

Blair, W. F. (1941). Observations on the life history of *Baiomys taylori subater*. *J. Mammal.* **22**, 378-383. doi:10.2307/1374930

Borgard, H. L., Baab, K., Pasch, B. and Riede, T. (2019). The shape of sound: a geometric morphometrics approach to laryngeal functional morphology. *J. Mammal. Evol.* doi:10.1007/s10914-019-09466-9

Bradbury, J. W. and Vehrencamp, S. L. (2011). *Principles of Animal Communication*, 2nd edn. Sunderland, MA: Sinauer Associates.

Brudzynski, S. M. (2018). *Handbook of Ultrasonic Vocalization. A Window into the Emotional Brain*, Vol. 25. Elsevier.

Brudzynski, S. M., Bihari, F., Ociepa, D. and Fu, X.-W. (1993). Analysis of 22 kHz ultrasonic vocalization in laboratory rats: long and short calls. *Physiol. Behav.* **54**, 215-221. doi:10.1016/0031-9384(93)90102-L

Campbell, P., Pasch, B., Pino, J. L., Crino, O. L., Phillips, M. and Phelps, S. (2010). Geographic variation in the songs of Neotropical singing mice: testing the relative importance of drift and local adaptation. *Evolution* **64**, 1955-1972. doi:10.1111/j.1558-5646.2010.00962.x

Campbell, P., Arévalo, L., Martin, H., Chen, C., Sun, S., Rowe, A. H., Webster, M. S., Searle, J. B. and Pasch, B. (2019). Vocal divergence is concordant with genomic evidence for strong reproductive isolation in grasshopper mice (Onychomys). *Ecol. Evol.* **9**, 12886-12896. doi:10.1002/ece3.5770

Carleton, M. D. (1980). Phylogenetic relationships in neotomine–peromyscine rodents (Muroidea) and a reappraisal of the dichotomy within New World Cricetinae. *Misc. Publ. Mus. Zool. Univ. Mich.* **157**, 1-146.

deBoer, B. (2009). Acoustic analysis of primate air sacs and their effect on vocalization. *J. Acoust. Soc. Am.* **126**, 3329-3335.

Dent, M. L., Fay, R. R. and Popper, A. N. (2018). Rodent bioacoustics. In *Springer Handbook of Auditory Research*, vol. 67. Springer.

Eliason, C. M., Maia, R. and Shawkey, M. D. (2015). Modular color evolution facilitated by a complex nanostructure in birds. *Evolution* **69**, 357-367. doi:10.1111/evo.12575

Eliason, C. M., Maia, R., Parra, J. L. and Shawkey, M. D. (2020). Signal evolution and morphological complexity in hummingbirds (Aves: Trochilidae). *Evolution* **74**, 447-458. doi:10.1111/evo.13893

Eshelman, B. D. and Cameron, G. N. (1987). *Baiomys taylori*. *Mamm. Species*, 1-7. doi:10.2307/3503776

Grimsley, J. M. S., Sheth, S., Vallabh, N., Grimsley, C. A., Bhattal, J. and Latsko, M. (2016). Contextual modulation of vocal behavior in mouse: newly identified 12 kHz "mid-frequency" vocalization emitted during restraint. *Front. Behav. Neurosci.* **10**, 38. doi:10.3389/fnbeh.2016.00038

Hooper, E. T. and Carleton, M. D. (1976). Reproduction, growth and development in two contiguously allopatric rodent species, genus *Scotinomys*. *Misc. Publ. Mus. Zool. Univ. Mich.* **151**, 1-52.

Holy, T. E. and Guo, Z. (2005). Ultrasonic songs of male mice. *PLoS Biol.* **3**, e386. doi:10.1371/journal.pbio.0030386

Kalcounis-Rueppell, M. C., Petric, R., Briggs, J. R., Carney, C., Marshall, M. M., Willse, J. T., Rueppell, O., Ribble, D. O. and Crossland, J. P. (2010). Differences in ultrasonic vocalizations between wild and laboratory California mice (*Peromyscus californicus*). *PLoS ONE* **5**, e9705. doi:10.1371/journal.pone.0009705

Kalcounis-Rueppell, M. C., Petric, R. and Marler, C. A. (2018). The bold, silent type: predictors of ultrasonic vocalizations in the genus *Peromyscus*. *Front. Ecol. Evol.* **6**, 198. doi:10.3389/fevo.2018.00198

King, A. S. and McLelland, J. (1984). *Birds: Their Structure and Function*, pp. 28-42. London: Bailliere Tindall.

Light, J. E., Ostroff, M. O. and Hafner, D. J. (2016). Phylogeographic assessment of the northern pygmy mouse, *Baiomys taylori*. *J. Mammal.* **97**, 1081-1094. doi:10.1093/jmammal/gyw065

Miller, J. R. and Engstrom, M. D. (2007). Vocal stereotypy and singing behavior in Baiomyine mice. *J. Mammal.* **88**, 1447-1465. doi:10.1644/06-MAMM-A-386R.1

Miller, J. R. and Engstrom, M. D. (2010). Stereotypic vocalizations in harvest mice (*Reithrodontomys*): Harmonic structure contains prominent and distinctive audible, ultrasonic, and non-linear elements. *J. Acoust. Soc. Am.* **128**, 1501-1512. doi:10.1121/1.3455855

Miller, J. R. and Engstrom, M. D. (2012). Vocal stereotypy in the rodent genera *Peromyscus* and *Onychomys* (Neotominae): taxonomic signature and call design. *Bioacoustics* **21**, 193-213. doi:10.1080/09524622.2012.675176

Negus, V. E. (1949). *The Comparative Anatomy and Physiology of the Larynx*. New York: Grune&Stratton, Inc.

Nowicki, S. (1987). Vocal tract resonances in oscine bird sound production: evidence from birdsongs in a helium atmosphere. *Nature* **325**, 53-55. doi:10.1038/325053a0

Okobi, D. E., Jr, Banerjee, A., Matheson, A. M. M., Phelps, S. M. and Long, M. A. (2019). Motor cortical control of vocal interaction in neotropical singing mice. *Science* **363**, 983-988. doi:10.1126/science.aau9480

Ord, T. J., Collar, D. C. and Sanger, T. J. (2013). The biomechanical basis of evolutionary change in a territorial display. *Func. Ecol.* **27**, 1186-1200. doi:10.1111/1365-2435.12110

Packard, R. L. (1960). Speciation and evolution of the pygmy mice, genus *Baiomys*. *Univ. Kans. Publ. Mus. Nat. Hist.* **9**, 579-670. doi:10.5962/bhl.part.6498

Pasch, B., George, A. S., Hamlin, H. J., Guillette, L. J. and Phelps, S. M. (2011). Androgens modulate song effort and aggression in Neotropical singing mice. *Horm. Behav.* **59**, 90-97. doi:10.1016/j.yhbeh.2010.10.011

Pasch, B., Bolker, B. M. and Phelps, S. M. (2013). Interspecific dominance via vocal interactions mediates altitudinal zonation in neotropical singing mice. *Am. Nat.* **182**, E161-E173. doi:10.1086/673263

Pasch, B., Tokuda, I. T. and Riede, T. (2017). Grasshopper mice employ distinct vocal production mechanisms in different social contexts. *Proc. R. Soc. Lond. B* **284**, 20171158. doi:10.1098/rspb.2017.1158

Riede, T. (2013). Stereotypic laryngeal and respiratory motor patterns generate different call types in rat ultrasound vocalization. *J. Exp. Zool. A* **319**, 213-224. doi:10.1002/jez.1785

Riede, T. (2018). Peripheral vocal motor dynamics and combinatory call complexity of ultrasonic vocal production in rats. In *Handbook of Ultrasonic Vocalization*, Vol. 25: series 'Handbook of Behavioral Neuroscience' (ed. S. M. Brudzynski), pp. 45-60: Elsevier.

Riede, T., Tokuda, I. T., Munger, J. B. and Thomson, S. L. (2008). Mammalian laryngseal air sacs add variability to the vocal tract impedance: physical and computational modeling. *J. Acoust. Soc. Am.* **124**, 634-647.

Riede, T., Borgard, H. L. and Pasch, B. (2017). Laryngeal airway reconstruction indicates that rodent ultrasonic vocalizations are produced by an edge-tone mechanism. *R. Soc. Open Sci.* **4**, 170976. doi:10.1098/rsos.170976

Sales, G. D. and Pye, D. (1974). *Ultrasonic Communication by Animals*. London: Chapman & Hall.

Schneider, R. (1964). Der Larynx der Säugetiere. *Handb. der Zool.* **5**, 1-128.

Sikes, R. S. and The Animal Care and Use Committee of the American Society of Mammalogists (2016). Guidelines of the American Society of Mammalogists for the use of wild mammals in research and education. *J. Mammal.* **97**, 663-688.

Spencer, M. L. and Titze, I. R. (2001). An investigation of a modal-falsetto register transition hypothesis using helox gas. *J. Voice* **15**, 15-24. doi:10.1016/S0892-1997(01)00003-0

Sundberg, J. (1981). Formants and fundamental frequency control in singing. An experimental study of coupling between vocal tract and vocal source. *Acoustica* **49**, 48-54.

Titze, I., Riede, T. and Mau, T. (2016). Predicting achievable fundamental frequency ranges in vocalization across species. *PLoS Comput. Biol.* **2**, e1004907. doi:10.1371/journal.pcbi.1004907

Tschida, K., Michael, V., Takatoh, J., Han, B.-X., Zhao, S., Sakurai, K., Mooney, R. and Wang, F. (2019). A specialized neural circuit gates social vocalizations in the mouse. *Neuron* **103**, 459-472.e4. doi:10.1016/j.neuron.2019.05.025

Wilson, D. E. and Reeder, D. M. (2005). *Mammal Species of the World: A Taxonomic and Geographic Reference*, 3rd edn. Baltimore, MD: Johns Hopkins University Press.

Wolak, M. E., Fairbairn, D. J. and Paulsen, Y. R. (2012). Guidelines for estimating repeatability. *Methods Ecol. Evol.* **3**, 129-137. doi:10.1111/j.2041-210X.2011.00125.x

Wright, J. M., Gourdon, J. C. and Clarke, P. B. S. (2010). Identification of multiple call categories within the rich repertoire of adult rat 50-kHz ultrasonic vocalizations: effects of amphetamine and social context. *Psychopharmacology* **211**, 1-13. doi:10.1007/s00213-010-1859-y

Zelditch, M. L., Lundrigan, B. L. and Garland, T., Jr. (2004). Developmental regulation of skull morphology. I. Ontogenetic dynamics of variance. *Evol. Dev.* **6**, 194-206. doi:10.1111/j.1525-142X.2004.04025.x

Zhang, Y. S. and Ghazanfar, A. A. (2018). Vocal development through morphological computation. *PLoS Biol.* **16**, e2003933. doi:10.1371/journal.pbio.2003933